Journal of Engineering and Applied Sciences 13 (Special Issue 14): 10882-10887, 2018
ISSN: 1816-949X

Investigate the Influence of Ge Addition on the Corrosion Resistance and Microstructure of Cu-Al-Ni Shape Memory Alloy Prepared via. Powder Metallurgy

Ali H. Haleem and Hussein A. Hashim
Department of Metallurgical Engineering, College of Materials Engineering,
University of Babylon, Hillah, Iraq

Abstract: The effect of different amounts (1, 2 and 3% wt.) of Ge additions on the corrosion behavior and microstructure of Cu-Al-Ni SMA were investigated by SEM, XR, EDS and electrochemical test. It was found that the microstructure and corrosion characteristics are highly sensitive to the composition changes. It was observed that the germanium addition controlled. The phase morphology along with the formation of Ge rich precipitates with copper which is (Cu_3 Ge and CuGe). The corrosion behavior of the Cu-Al-Ni SMA before and after the germanium addition were studied by electrochemical tests in 3.5% NaCl. solution. It was noticed that the corrosion rate of Cu-Al-Ni SMA in 3.5% NaCl was (34.99 mpy) and when added 3% Ge the corrosion rate decrease to become (4.72 mpy). This improved that the alloy containing higher amount of Ge has excellent properties than the base alloy. The confederation of XRD together with SEM and EDX showed that the corrosion products Ge_4Na and Al_2O_3 represent as a protective layers which enhance the corrosion resistance of Cu-Al-Ni-Ge SMA.

Key words: Cu-Al-Ni alloy, powder metallurgy, electrochemical test, SMA, microstructure, XRD

INTRODUCTION

The term Shape Memory Alloys (SMA) is applied to that group of metallic materials that demonstrate the ability to return to some previously defined shape or size when subjected to the appropriate thermal procedure (Hodgson, 1988). The properties of shape memory effect are function of microstructure which including texture, grain size and precipitations occurs (Tatar and Zengin, 2005). Many research were presented to improve the Properties of this alloy. Kuo *et al*. (2006) studied "the corrosion behavior of Cu-Al-Ni shape-memory alloys in 0.5 mL H_2SO_4 solution at 25°C which studied by means of anodic polarization and cyclic voltammeter and the results showed that anodic dissolution rates of alloys decreased slightly with increasing the concentrations of aluminum, however, the formation of barrier film of Al_2O_3 on the alloy surface was the main reason for the improvement of corrosion resistance of Cu-Al-Ni alloy" (Badawy *et al*., 2014). Ali and Al-Tai (2010) have studied "the effect of iron addition on the corrosion behavior of Cu-Al-Ni shape memory alloy in 5% NaOH and different amount of Fe (0.4, 0.8, 1.2 wt.%) their results showed that the Cu-Al-Ni shape memory alloy in austenitic structure has better corrosion resistance than in the martensitic structure and the higher corrosion resistance achieved when the Fe addition was 0.4%". Gojic *et al*. (2011) have studied "electrochemical and microstructural of Cu-Al-Ni SMA the corrosion behavior of Cu-Al-Ni shape memory alloy in 0.5 mL NaCl solution was investigated by linear and open circuit potential measurements. The results have shown that the adsorption of chloride ions on the electrode surface leads to the decrease of EOCP values and the breakdown of the protective surface oxide film". Saud *et al*. (2017) study "the effect of Ta additions on the microstructure, damping, corrosion resistance and shape memory behavior of prealloyed Cu-Al-Ni shape memory alloys. Polarization tests in 3.5% NaCl solution showed that the corrosion resistance of Cu-Al-Ni-Ta SMA improved with escalating Ta concentration, higher corrosion potential and formation of stable passive film". The purpose of this study was to investigate the corrosion resistance and microstructure of Cu-Al-Ni SMA with different contents of Ge additions (1, 2 and 3 wt.%) in a 3.5% NaCl solution. Study the corrosion resistance in 3.5% NaCl for Cu-Al-Ni SMA prepared by powder metallurgy with addition of (1, 2 and 3 wt.%) of germanium have not been reported elsewhere.

Experimental procedure

Sample preparation: The samples are produced by powder metallurgy technique using an elemental powders

Corresponding Author: Ali H. Haleem, Department of Metallurgical Engineering, College of Materials Engineering, University of Babylon, Hillah, Iraq

Table 1: Elemental powders specification and composition

Properties	Cu	Al	Ni	Ge
Particle size (μm)	14.00	15.00	27.000	8
Purity (%)	99.95	99.92	99.950	99.94
Composition (wt.%)	83.60	11.90	4.500	-
	82.60	11.90	4.500	1
	81.60	11.90	4.500	2
	80.60	11.90	4.500	3

Cu-Al-Ni-Ge. Table 1 shows the particle size, purity and composition of the powders. The elemental powders are mixed using planetary ball mill for about 6 h with mixing ratio 1:5 by weight and rotation speed 350 rpm, 0.5 cc ethyl alcohol are used to reduce the temperature initiated from mixing which lead to oxidation of powder. Then the mixed powder are compacted by hydraulic press with 750 MPa using cylindrical stainless steel die with 10 mm as diameter. After that the green samples were inserted in vacuum furnace for about 120 min at 550°C and continue the sintering at 850°C for about 100 min with heating rate 10°C/min. The sintered specimens were heated at 900°C for 60 min and then quenched directly in iced water, followed by heating the sample to 300°C for 30 min in order to age intermetallic compound (γ_2) and to stabilize the martensite phase.

Preparation of specimens for microstructure observation: After the sintering, quenching and aging treatment, the specimens has been wet grinding using 180, 400, 800, 1000, 1200, 1500, 2000, 2500, 3000 grit silicon carbide papers using grinding wheel machine and then polishing by using polishing paper and diamond with 1-3 μm particle size. These samples are then cleaned with distilled water and dried with hot air after that the samples are then etched with etching solution is 2.5 g $FeCl_3$. $6H_2O$+48 mL CH_3OH+10 mL HCl, ferric chloride acid/methanol/hydrochloric acid, etching time is 10 sec and then use for SEM observation.

MATERIAL AND METHODS

Sample with dimensions (d = 10 mm, t = 5 mm) was used for X-ray diffraction characteristics using XRD type mini flex2. X-ray generator with CuKα radiation at 30.0 mA and 40.0 kV is used, the instrument was held at scan speed (2°/min), angles 2θ range between 30-90° with step 0.02°/sec. After XRD analysis, fillings of the alloy have been extracted for about 5-15 mg approximately. They were taken for differential scanning calorimeter test using DSC type I-series, the scanning rate was 5°C/min and the temperature range is 100-400°C.

Electrochemical test: The corrosion behavior of Cu-Al -Ni SMA after and before (1, 2 and 3%) germanium addition was achieved at 25°C in open air within a glass cell involve 350 mL of 3.5% NaCl (3.5 g NaCl+96.5 mL distillation water). The corrosion behavior of alloys has been investigated by Tafel potentiostatic type Wenking M lap to estimate corrosion current and corrosion potential.

Three electrodes was used for potentiodynamic polarization test. Platinum wire was considered as The counter electrode and the reference electrode was the Saturated Calomel Electrode (SCE) while the sample was the working electrode. Polarization curves were measured potentiostatically at a scan rate of 0.35 mVs^{-1}. For each measure, the electrodes were maintained at open circuit during at least (10-20 min) for stabilization and E_o has been obtained. Measurements the open circuit potential were performed to obtain some information about the evolution of the corrosion process. The corrosion current has been estimated from intersection of tangential of anode curve and cathode curve.

RESULTS AND DISCUSSION

Microstructure, X-ray diffraction for phase analysis and transformation temperature of CU-AL-NI SMAs after and before ge addition: The transformation temperatures of Cu-Al-Ni after and before addition of (1, 2 and 3%) Ge were determined in DSC test and the results were given in Table 2. From the table it was noted that the transformation temperatures of the alloy varied according to amount of Ge element added to the alloy. The highest transformation temperature was achieved when the addition was 3% Ge. The changes of the transformation temperatures take place due to the different type and shape of the martensite phas. Furthermore, the type and amount of the precipitates and intermetallic compounds which is Cu_9Al_4, $AlCu_4$, $AlNi_3$, CuGe, Cu_3 Ge might have influence on the transformation temperatures of the alloy.

Scanning electron microscope observation used in order to examine the influence of Ge addition on the microstructure of the alloy. After sintering the microstructure has only (Sold solution of Cu with Al) and γ_2 (Cu_9Al_4) phases and after direct quench the microstructure involve full martensite structure and there is no precipitation of γ_2 in the microstructure. Figure 1 shows the microstructure of Cu-Al-Ni SMA after Aging with germanium addition. It was noticed that, the microstructures obtained from SEM were all in martensitic structure at 25°C with needle like and platelet like shapes and there is also precipitation of γ_2 on the microstructure which proved by XRD test. The martensite shapes are indicate to two types of thermal induced martensite

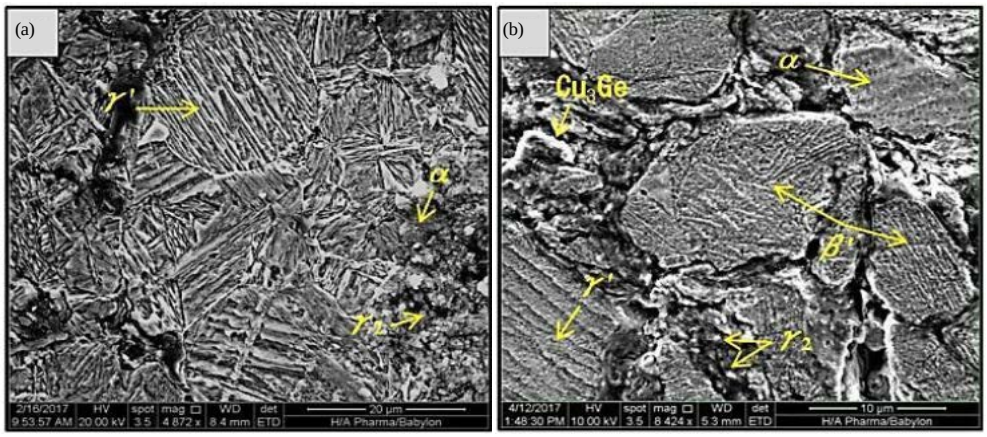

Fig. 1: a) SEM microstructure of Cu-Al-Ni SMA and b) SEM microstructure of Cu-Al-Ni-2% Ge SMA

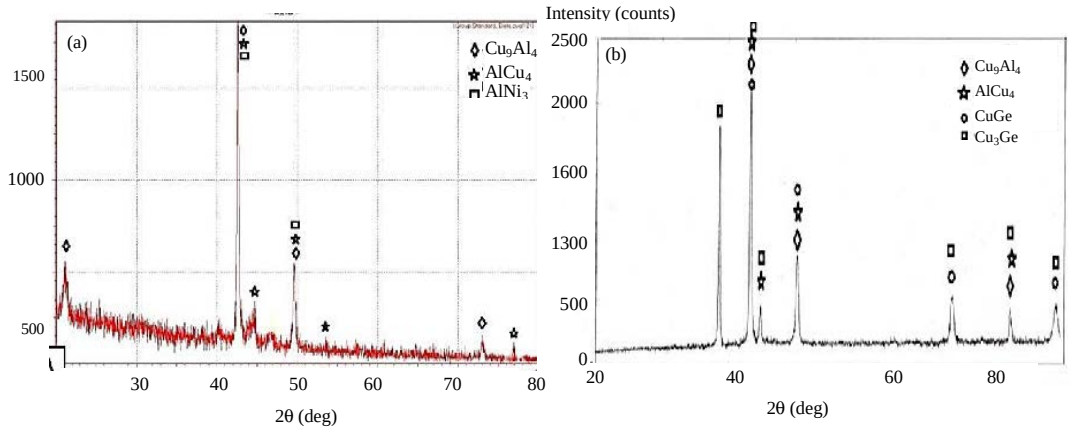

Fig. 2: a) XRD test results of Cu-Al-Ni SMA and b) XRD test results of Cu-Al-Ni-3% Ge SMA

Table 2: Transformation temperatures of Cu-Al-Ni SMA after and before Ge addition

	Transformation temperatures (°C)			
Alloy composition	A_S	A_F	M_S	M_F
Cu-Al-Ni	225	265	269	260
Cu-Al-Ni-1% Ge	227	268	270	263
Cu-Al-Ni-2% Ge	230	270	275	265
Cu-Al-Ni-3% Ge	253	272	275	269

which is β' and γ' phases where β' formed as needle like shape and γ' formed as coarse platelet like phase. "The needle-like β' martensite phase has very high thermo-elastic behaviour which can be attributed to their controlled growth in the self-accommodating groups" (Sari, 2010). Nevertheless, the microstructure of the alloy containing Ge addition present a self-accommodation plate like martensite in all aditions with some needle like phases as shown in Fig. 1b while the base alloy had plate like phases as shown in Fig. 1a. These platelet like and needle like martensite phases nucleated and grew in different orientations. The growth process of martensite phase involves the accommodation of the local stress field and therefore, it requires forming other groups (Sari, 2010).

Figure 2 shows the XRD results of the Cu-Al-Ni and Cu-Al-Ni-3% Ge SMAs. It was found that there is intermetallic compounds which is Cu_9Al_4, $AlCu_4$, $AlNi_3$ appears in the base alloy as shown in Fig. 2a and with Germanium addition extra intermetallic compounds appear which is CuGe and Cu_3 Ge as shown in Fig. 2b. It was noticed that the peaks of the patterns after and before the addition had a little difference in their shape and intensity and this is caused by the germanium addition. The common intermetallic compounds created in the Cu-Al-Ni SMA is Al_4Cu_9 and $AlCu_4$ which is also, appear in the Cu-Al-Ni-3% Ge SMA but in different amount and distribution.

Electrochemical test result: Figure 3 displays the polarization carves of Cu-Al-Ni SMA after and before

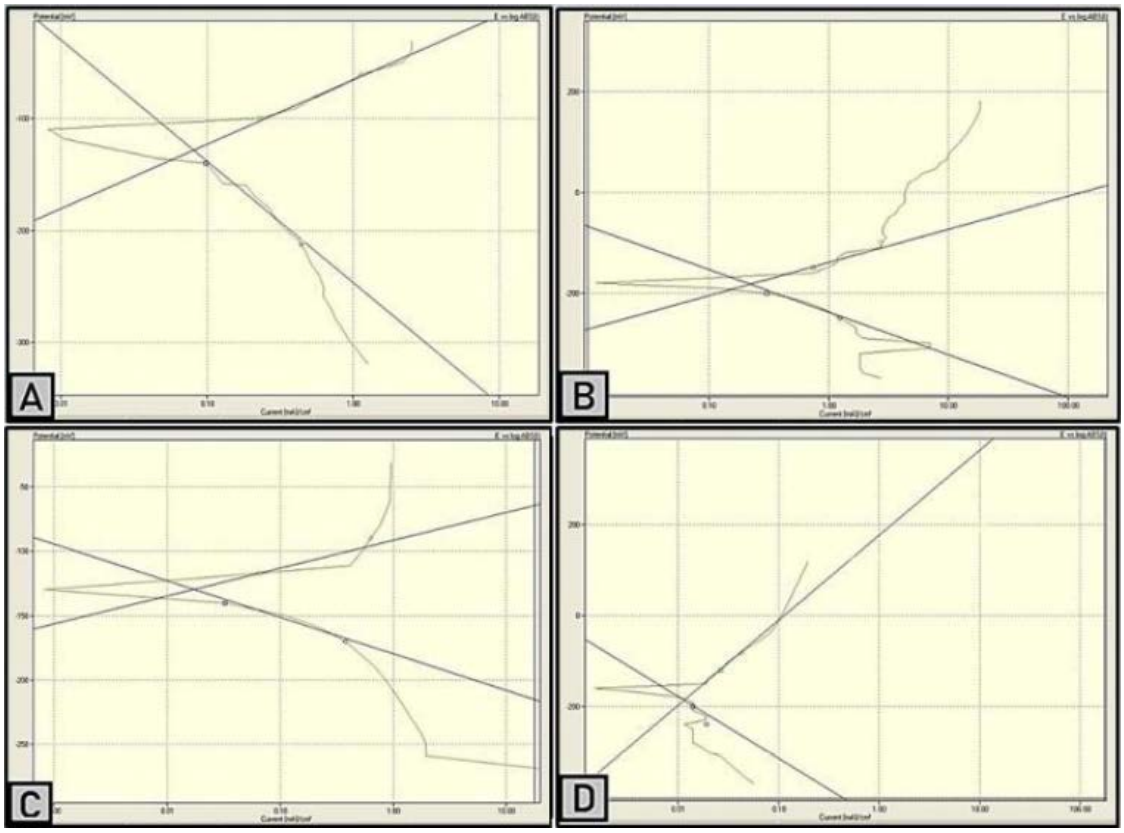

Fig. 3: a) The polarization carves for Cu-Al-Ni SMA; b) The polarization carves for Cu-Al-Ni-1%Ge SMA; c) The polarization carves Cu-Al-Ni-2%Ge SMA and d) The polarization carves Cu-Al-Ni-3% Ge SMA

Table 3: The polarization parameters of Cu-Al-Ni SMA in 3.5% NaCl solution after and before Ge addition

Alloy composition	Corrosion potential E_{corr} (mV)	Current density I_{corr} (μA/cm^2)	Corrosion rate (mpy)
Cu-Al-Ni	-128.5	80.98	34.99
Cu-Al-Ni-1% Ge	-182.5	21.48	09.14
Cu-Al-Ni-2% Ge	-129.6	17.26	07.23
Cu-Al-Ni-3% Ge	-186.2	11.43	04.72

(1, 2 and 3%) Ge addition. Cu-Al-Ni SMA decreases anodic polarization tendency while improving the cathodic polarization performance (Chen *et al*., 2005). The presence of Ge in the passivation layer enhance the resistance of the alloy from the aggressive action of Cl^- in the NaCl solution better than the alloy does not contain Ge element (Kassab *et al*., 2014). The corrosion rate (mpy), corrosion potential (E_{cor}) and corrosion current density (I_{corr}) of samples calculated from the polarization curves presented in Table 3. The corrosion current (I_{corr}) is associated with corrosion rate (mpy) through the following empirical equations:

$$C.R(mpy) = \frac{0.13 \times I_{corr} \times E.W}{A \times \rho} \quad (1)$$

Where:

A = Area of the surface (cm^2)
ρ = Density of the sample (g/cm^2)
I_{corr} = Corrosion current density (μA/cm^2)
EW = Equivalent Weight

From Table 3, the corrosion rate (mpy) of the Cu-Al-Ni SMA is (34.99 mpy) and with addition of (1, 2 and 3%) Ge the corrosion rate become (9.14, 7.23 and 4.72 mpy), respectively. The formation of corrosion products (Ge_4Na and Al_2O_3) as shown in X-ray diffraction after corrosion in 3.5% NaCl as shown in Fig. 4 is the reason for decreases the corrosion rate from (34.99 mpy) in Cu-Al-Ni SMA to (4.72 mpy) in Cu-Al-Ni-3% Ge SMA. For most applications, corrosion penetration rate less than about (20 mpy) is acceptable (Callister, 1991). Figure 5 shows the Energy Dispersive X-ray spectroscopy (EDX) analysis of Cu-Al-Ni SMA after corrosion in 3.5% NaCl solution. The EDX peaks of the elements located on the sample surface were shown in Fig. 5a and the chemical composition of these elements were shown in Fig. 5b.

Figure 6 shows the EDX analysis of Cu-Al-Ni-3% Ge SMA after corrosion test in 3.5% NaCl solution. The EDX

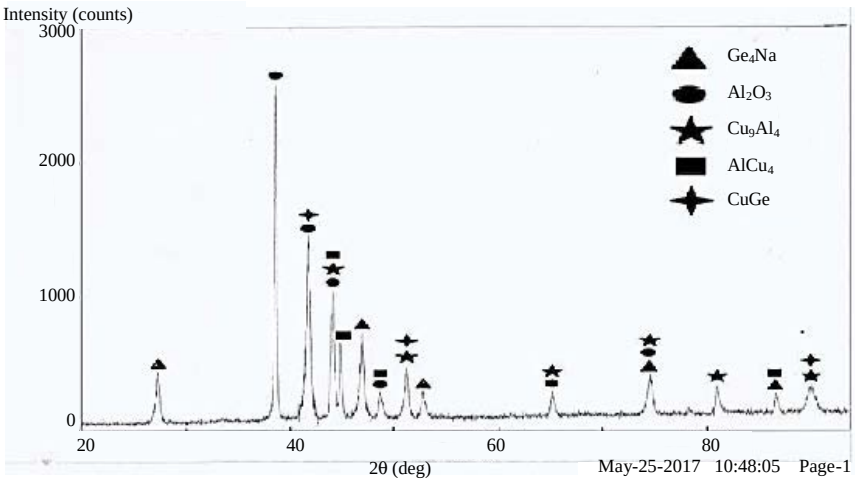

Fig. 4: The XRD pattern for Cu-Al-Ni-3% Ge after corrosion test in 3.5% NaCl solution

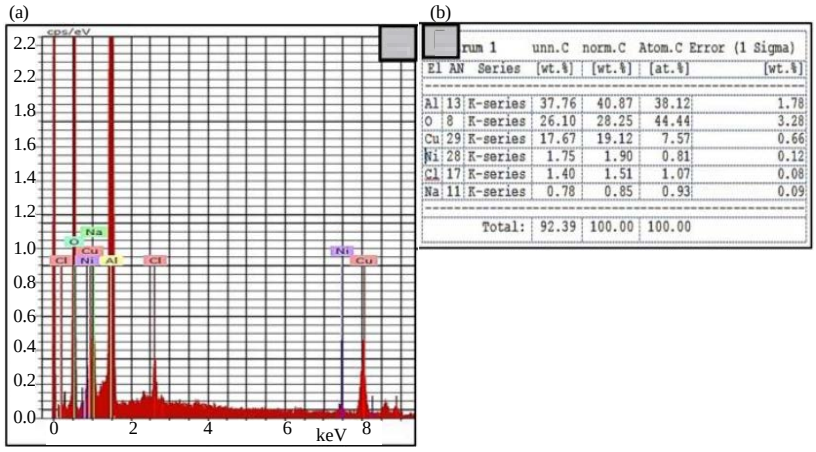

Fig. 5: The EDX analysis of Cu-Al-Ni SMA: a) EDX peaks of the elements and b) Chemical composition of the elements

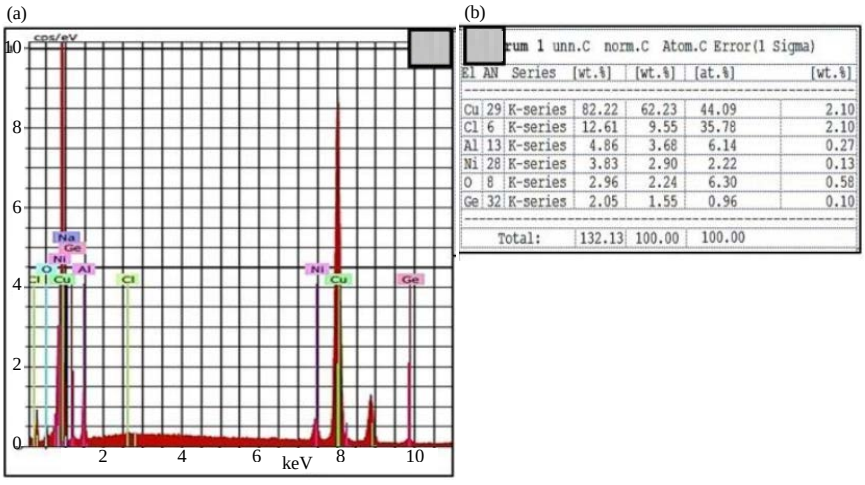

Fig. 6: The EDX analysis of Cu-Al-Ni-3% Ge SMA: a) EDX peaks of the elements and b) Chemical composition of the elements

peaks of the elements located on the sample surface were shown in Fig. 6a and the chemical composition of these elements were shown in Fig. 6b. The Cl-Na and O elements on the surface of the sample is indicated to the formation of corrosion products. The presence of O element as shown in the EDX analysis is indicated to the formation of oxides such as Cu_2O and Al_2O_3 which represent the protective layer.

CONCLUSION

It was found that the martensitic and austenitic transformation temperatures were changed according to the alloy composition and germanium addition. It was noticed that the highest transformation temperature achieved when we added 3% Ge. The electrochemical test shows that the corrosion rate decrease from 34.99-4.72 (mpy) when the addition of germanium is 3%. we concluded that increase the germanium addition lead to improve the corrosion resistance of Cu-Al-Ni SMA.

REFERENCES

Ali, A.R.K.A. and Z.T.K. Al-Tai, 2010. The effect of Iron addition on the dry sliding wear and corrosion behavior of Cu-Al-Ni shape memory alloy. Eng. Technol. J., 28: 6888-6902.

Badawy, W.A., M.M. El-Rabiei and H. Nady, 2014. Synergistic effects of alloying elements in Cu-ternary alloys in chloride solutions. Electrochim. Acta, 120: 39-45.

Callister, W.D., 1991. Materials Science and Engineering: An Introduction. 5th Edn., John Wiley & Sons, Hoboken, New Jersey, USA., ISBN:9780471320135, Pages: 896.

Chen, B., C. Liang, D. Fu and D. Ren, 2005. Corrosion behavior of Cu and the Cu-Zn-Al shape memory alloy in simulated uterine fluid. Contraception, 72: 221-224.

Gojic, M., L. Vrsalovic, S. Kozuh, A. Kneissl and I. Anzel *et al*., 2011. Electrochemical and microstructural study of Cu-Al-Ni shape memory alloy. J. Alloys Compd., 509: 9782-9790.

Hodgson, D.E., 1988. Using shape memory alloys. Shape Memory Applications, San Jose, California, USA.

Kassab, E., L. Neelakantan, M. Frotscher, S. Swaminathan and B. Maaß *et al*., 2014. Effect of ternary element addition on the corrosion behaviour of NiTi shape memory alloys. Mater. Corros., 65: 18-22.

Kuo, H.H., W.H. Wang, Y.F. Hsu and C.A. Huang, 2006. The corrosion behavior of Cu-Al and Cu-Al-Be shape-memory alloys in $0.5MH_2SO_4$ solution. Corros. Sci., 48: 4352-4364.

Sari, U., 2010. Influences of 2.5 wt% Mn addition on the microstructure and mechanical properties of Cu-Al-Ni shape memory alloys. Intl. J. Miner. Metall. Mater., 17: 192-198.

Saud, S.N., E. Hamzah, H.R. Bakhsheshi-Rad and T. Abubakar, 2017. Effect of Ta additions on the microstructure, damping and shape memory behaviour of Prealloyed Cu-Al-Ni shape memory alloys. Scanning, 2017: 1-13.

Tatar, C. and R. Zengin, 2005. The effects of ã-irradiation on some physical properties of Cu-13.5 wt.% Al-4 wt.% Ni shape memory alloy. Mater. Lett., 59: 3304-3307.